10-2002

# Real-time in vivo imaging of platelets, tissue factor and fibrin during arterial thrombus formation in the mouse

Shahrokh Falati

Peter Gross

Glenn Merrill-Skoloff

Barbara C. Furie

Bruce Furie

# Real-time *in vivo* imaging of platelets, tissue factor and fibrin during arterial thrombus formation in the mouse

SHAHROKH FALATI, PETER GROSS, GLENN MERRILL-SKOLOFF, BARBARA C. FURIE & BRUCE FURIE

*Center for Hemostasis and Thrombosis Research, Beth Israel Deaconess Medical Center and Harvard Medical School, Boston, Massachusetts 02215, USA*

*Correspondence should be addressed to B.F.; email: bfurie@caregroup.harvard.edu*

Published online: 16 September 2002, doi:10.1038/nm782



**We have used confocal and widefield microscopy to image thrombus formation in real time in the microcirculation of a living mouse. This system provides high-speed, near-simultaneous acquisition of images of multiple fluorescent probes and of a brightfield channel. Vascular injury is induced with a laser focused through the microscope optics. We observed platelet deposition, tissue factor accumulation and fibrin generation after laser-induced endothelial injury in a single developing thrombus. The initiation of blood coagulation *in vivo* entailed the initial accumulation of tissue factor on the upstream and thrombus–vessel wall interface of the developing thrombus. Subsequently tissue factor was associated with the interior of the thrombus. Tissue factor was biologically active, and was associated with fibrin generation within the thrombus.**

Blood coagulation is a host defense mechanism that maintains the closed high-pressure circulatory system when blood-vessel integrity is compromised. Pathologic processes, including inflammation and atherosclerosis, are associated with thrombus formation. Occlusion of vessels and the resultant ischemia are a principal cause of morbidity and mortality. Despite advances in the understanding of platelet function, leukocyte adhesion, blood coagulation and fibrinolysis from *in vitro* experiments, knowledge of these processes *in vivo* has been limited by the lack of direct observational tools. We have developed instrumentation for imaging real-time thrombus formation in the microcirculation of a mouse using intravital high-speed confocal and widefield microscopy. This system provides nearly simultaneous acquisition of images of multiple fluorescent probes and of data through a brightfield channel, and can deliver a laser-induced injury through the microscope optics. With a laser-induced endothelial injury model[1], we have studied the assembly of platelets, tissue factor and fibrin during thrombus formation *in vivo* by fluorescence and brightfield microscopy. We used intravital microscopy to capture digital videos of thrombotic events.

### *In vivo* imaging during thrombus development

We infused fluorescent antibodies to label cellular and protein components in the blood of a living mouse. Upon induction of endothelial injury in a cremaster muscle arteriole, the accumulation of these antibodies in the developing thrombus can be detected, imaged and quantified. In our study antibodies directed against CD41, a platelet-specific antigen, accumulated in the thrombus (Fig. 1*a*). A brightfield image of the thrombus in the microcirculation, a fluorescence image of labeled platelets and a composite image showed the co-localization of platelets with the thrombus (Fig. 1*a*). When a control antibody was used, no accumulation of fluorochrome in the thrombus was seen (Fig. 1*a*). The integrated fluorescence intensity associated with the antibody against CD41 was significantly higher than that associated with the control antibody ($5.0 \times 10^6 \pm 1.2 \times 10^6$ as compared to $9.8 \times 10^4 \pm 0.5 \times 10^4$, average of ten independent experiments; $P = 0.0002$). Antibodies specific for fibrin also accumulated in the thrombus (Fig. 1*b*). A brightfield image, a fluorescence image and their composite showed co-localization of fibrin with the thrombus (Fig. 1*b*). Infusion with a control antibody resulted in minimal fluorochrome accumulation in the thrombus. Comparing the integrated fluorescence intensities associated with the antibody against fibrin and the control antibody showed that there was minimal non-specific accumulation of antibody within the thrombus (Fig. 1*b*). The integrated fluorescence intensity associated with the antibody against fibrin was significantly higher than that associated with the control antibody were ($3.4 \times 10^6 \pm 0.7 \times 10^6$ as compared to $3.3 \times 10^5 \pm 0.2 \times 10^5$, average of ten independent experiments; $P = 0.0011$).

Fluorescently labeled antibodies directed against tissue factor accumulated in the thrombus (Fig. 1*c*). A brightfield image, a fluorescence image and their composite image show the co-localization of tissue factor with the thrombus (Fig. 1*c*). A fluorescent control antibody did not accumulate in the thrombus. Comparing the integrated fluorescence intensities associated with the antibody against tissue factor and the control antibody showed limited non-specific incorporation of the irrelevant antibody into the thrombus. The integrated fluorescence intensity associated with the antibody against tissue factor was significantly higher than that associated with the control antibody ($5.9 \times 10^6 \pm 1.1 \times 10^6$ as compared to $2.0 \times 10^6 \pm 0.5 \times 10^6$, average of 12 independent experiments; ($P = 0.0025$). Parallel experiments using Fab fragments of the antibody against tissue factor yielded similar results (data not shown).

To examine the time course of platelet and fibrin accumulation in the developing thrombus, we labeled both platelets and fibrin with fluorescently labeled antibodies. Widefield fluorescence images of platelet and fibrin deposition and a brightfield image of the microcirculation showed co-localization of platelets and fibrin in the thrombus (Fig. 2*a*). The time course of platelet and fibrin accumulation in three separate experiments (Fig. 2*b*) showed that platelets accumulate rapidly and the thrombus enlarges, then diminishes in size. After a lag of about 15–20 seconds after endothelial injury, fibrin accumulated in the thrombus. Hirudin, an inhibitor of thrombin, prevented the generation of fibrin in the developing throm-

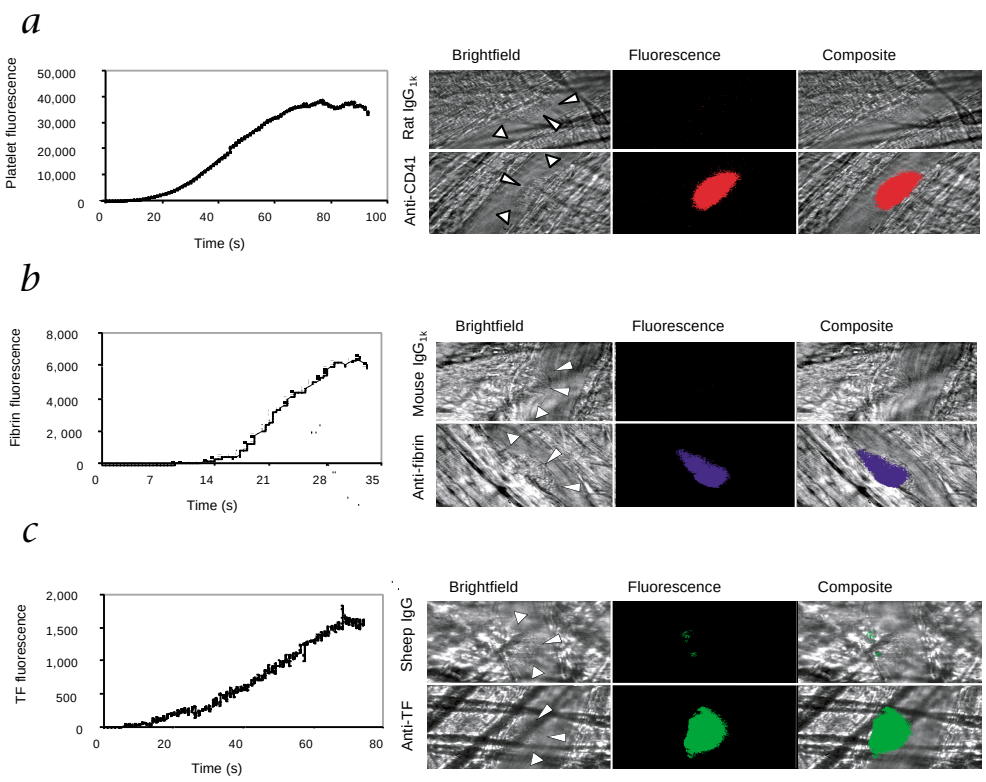


**Fig. 1** Imaging of platelets, fibrin and tissue factor in arterial thrombi using fluorescent antibodies. Incorporation of fluorescence signals into thrombi generated in wild-type mice was analyzed. Left, integrated fluorescence intensity over time for representative thrombi. Right, brightfield, fluorescence and composite images at 60 s after injury for specific (lower) or control (upper) antibody. Blood flow is from top to bottom. ***a***, Distribution of platelets, detected with purified rat antibody against mouse CD41 and Alexa 488–conjugated chicken anti-rat IgG. Purified rat $IgG_{1k}$ and Alexa 488–conjugated chicken anti-rat IgG were used in separate mice as control. ***b***, Distribution of fibrin, detected with purified mouse anti-human fibrin-specific antibody and Alexa 488–conjugated goat anti-mouse IgG. Mouse $IgG_{1k}$ and Alexa 488–conjugated goat anti-mouse IgG were used as control. ***c***, Distribution of tissue factor, detected with Alexa 488–labeled sheep anti-rabbit tissue factor antibodies. Alexa 488–labeled sheep IgG was used as control.

bus. Although the time course of tissue factor appearance was of interest, tissue factor is a trace protein, and the signal-to-noise level was too low for us to be certain of the timing of tissue factor detection relative to the detection of platelets and fibrin.

### Confocal imaging of the developing thrombus

Intravital confocal images of fibrin and platelets were generated to determine the distribution of these components. After endothelial injury, image sections of a thrombus were acquired at 1-μm intervals across the vessel diameter by incrementally altering the working distance between the microscope objective and the specimen with a piezo-electric driver. Representative sections are shown for a thrombus at about 60 seconds after injury (Fig. 3*a*). These confocal slices more accurately reveal the distribution of fibrin and platelets within the thrombus than do the widefield images. Fibrin appears with platelets near the top of the thrombus and shows significant co-localization with platelets, although its highest density is along the vessel wall and the upstream edge of the thrombus. Tissue factor is distributed widely in the thrombus, but is also concentrated along the throm-

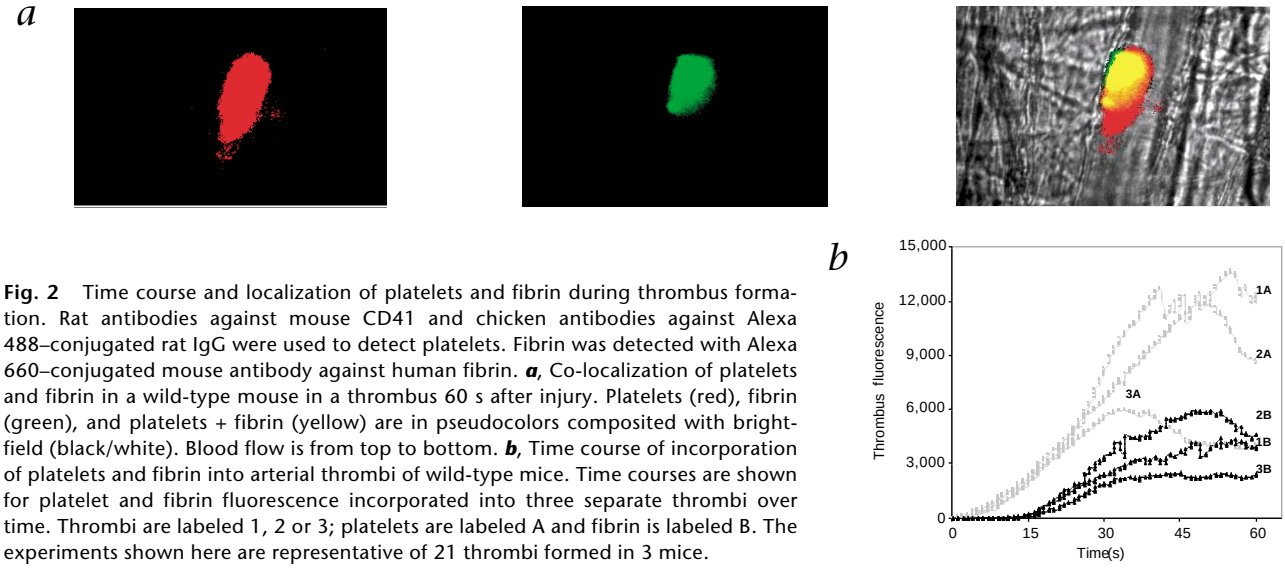


**Fig. 2** Time course and localization of platelets and fibrin during thrombus formation. Rat antibodies against mouse CD41 and chicken antibodies against Alexa 488–conjugated rat IgG were used to detect platelets. Fibrin was detected with Alexa 660–conjugated mouse antibody against human fibrin. ***a***, Co-localization of platelets and fibrin in a wild-type mouse in a thrombus 60 s after injury. Platelets (red), fibrin (green), and platelets + fibrin (yellow) are in pseudocolors composited with brightfield (black/white). Blood flow is from top to bottom. ***b***, Time course of incorporation of platelets and fibrin into arterial thrombi of wild-type mice. Time courses are shown for platelet and fibrin fluorescence incorporated into three separate thrombi over time. Thrombi are labeled 1, 2 or 3; platelets are labeled A and fibrin is labeled B. The experiments shown here are representative of 21 thrombi formed in 3 mice.

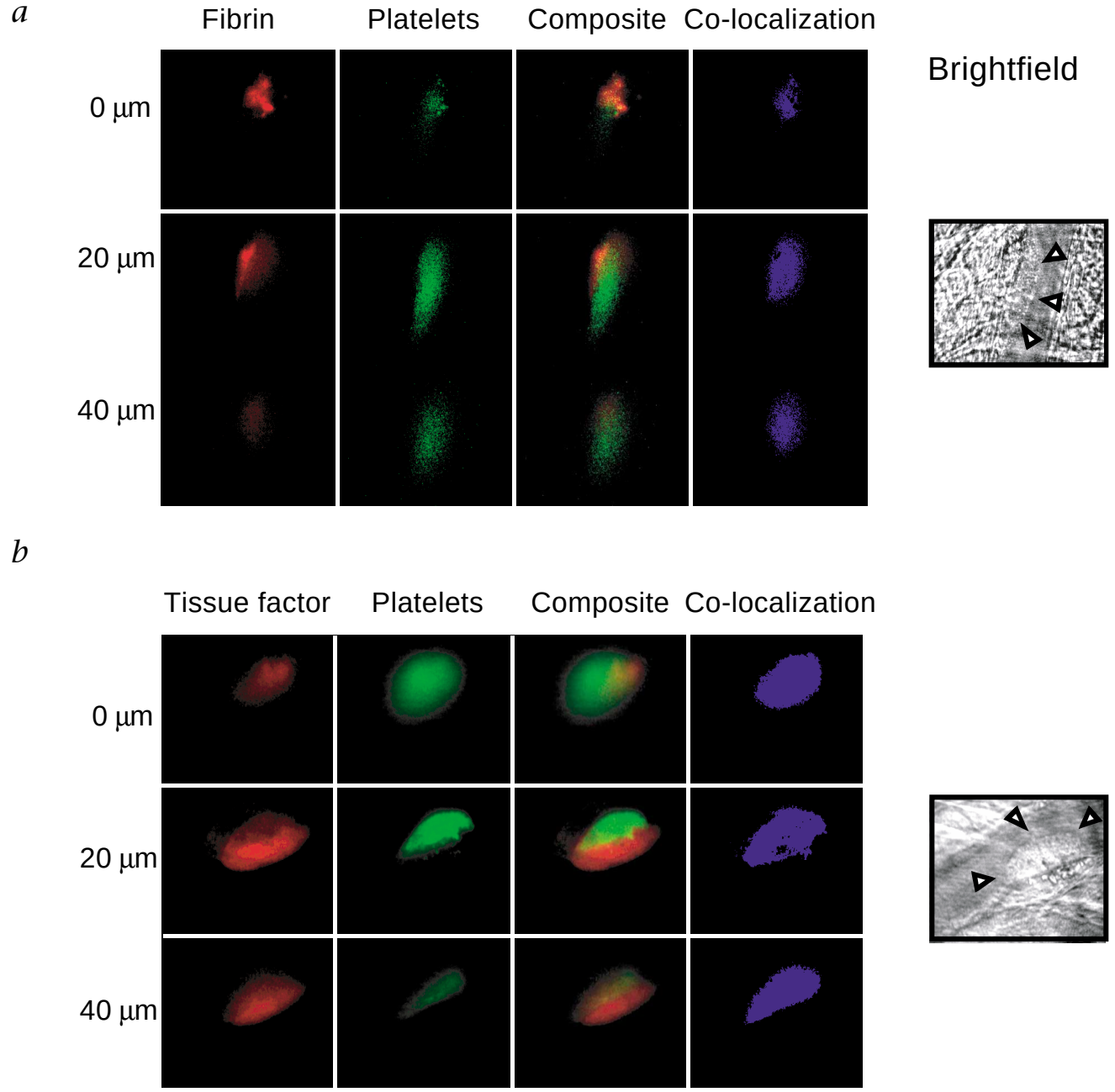


**Fig. 3** Confocal fluorescence imaging of the distribution of tissue factor, platelets and fibrin in a thrombus. Confocal images of a thrombus 60 s after injury were obtained by taking optical slices at 1-μm increments through approximately 80 μm. Images were collected in both the 488- and 647-nm channels. Representative optical slices at 20-μm intervals are shown. The panel labeled '20 μm' represents the approximate center of the thrombus. ***a***, Fibrin was detected with Alexa 660–conjugated mouse antibody against human fibrin, and platelets were detected using a combination of rat antibody against mouse CD41 and Alexa 488–conjugated chicken antibody against rat IgG. Arrowheads indicate thrombus surface exposed to flowing blood (brightfield image). Blood flow is from top to bottom. ***b***, In a thrombus 60 s after injury, platelets were imaged with Alexa 660–conjugated rat antibody against mouse CD41 Fab, and tissue factor was detected with Alexa 488–conjugated sheep antibody against rabbit tissue factor. The vessel wall is beneath the platelet thrombus (brightfield image). Blood flow is from right to left. Fibrin or tissue factor image: fibrin or tissue factor depicted as red pseudocolor with full dynamic range of intensity; platelet image, platelets depicted as green pseudocolor with full dynamic range of intensity; composite image, merge (yellow) of red and green fluorescence channel with full dynamic range of intensity; co-localization, all pixels containing both red and green signals are presented in blue, without modulation for intensity. Confocal images are representative of 12 thrombi formed in 2 mice.

bus–vessel wall interface and the upstream edge of the thrombus. In addition, although tissue factor and platelets co-localize, the density of tissue factor is greatest along the thrombus–vessel wall interface whereas the greatest density of platelets is above the vessel wall (Fig. 3*b*).

### Assembly of the developing thrombus

To compare the kinetics and localization of platelets, tissue factor and fibrin in the thrombus in a living mouse, we carried out intravital four-channel widefield fluorescence and brightfield imaging of these components (Fig. 4*a*). The composite

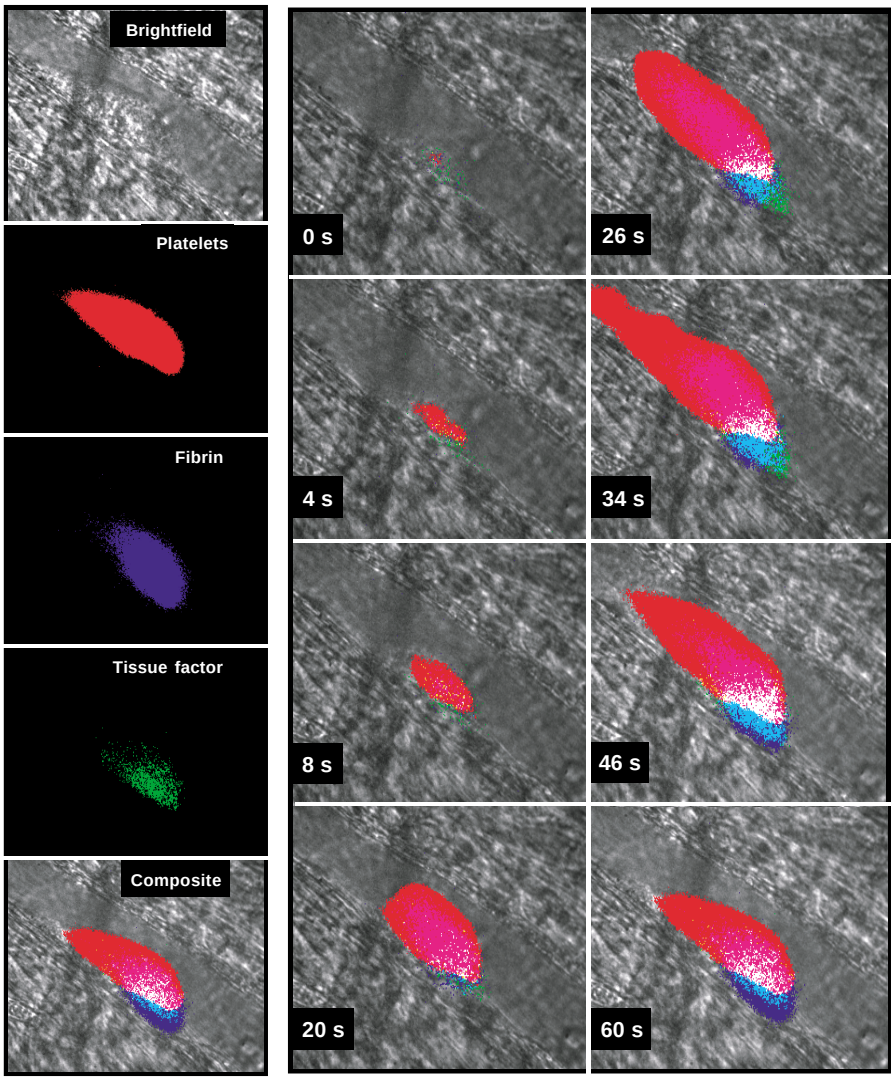


**Fig. 4** Structural organization during thrombus development. Intravital widefield imaging of platelet, tissue factor and fibrin deposition in the developing thrombus of a wild-type mouse after endothelial injury. Blood flow is from right to left. Alexa 660–conjugated CD41 Fab fragments, Alexa 488–conjugated sheep antibody against tissue factor and Alexa 350–conjugated mouse antibodies against human fibrin were infused into the systemic circulation. ***a***, Identification of thrombus components in four separate channels; black and white images are brightfield and pseudocolors represent the thrombus components. To simplify analysis of the composite image, the dynamic range of the intensity of each pseudocolor was minimized. ***b***, Composite images of the developing thrombus. Platelets (red); tissue factor (green); fibrin (blue); platelets + tissue factor (yellow); tissue factor + fibrin (turquoise); platelets + fibrin (magenta); platelets + fibrin + tissue factor (white). Using the fluorochromes, excitation filters and bandpass filters described, there was no crossover of fluorescence in each of the fluorescence channels. These images are representative of experiments producing a total of 14 thrombi in 3 mice. A videoclip of thrombus formation is available as Supplementary Movie 1 online.

four-channel image indicated that platelets are the principal component of the arterial thrombus. Fibrin was localized on the upstream edge of the thrombus and then extended through about 75% of the thrombus during the period examined. Tissue factor was localized on the upstream edge of the thrombus and along the vessel-wall interface.

We monitored assembly of the developing arterial thrombus by high-speed intravital four-channel imaging (Fig. 4*b*). At 0 seconds, the initial image immediately after injury showed minimal fluorescence. At 4 seconds, platelets accumulated on the vessel wall. Tissue factor was seen, but the signal-to-noise level was too low for us to be certain whether this initial signal was specific to tissue factor. As the platelet thrombus expanded at 20 seconds, fibrin appeared on the upstream edge of the thrombus. At 26 seconds, platelet thrombus expansion continued as the quantity of fibrin and tissue factor on the upstream edge increased, whereas fibrin and tissue factor extended distally in the thrombus. Between 34 and 60 seconds, fibrin extended through much of the platelet thrombus, although the downstream end of the thrombus remained exclusively composed of platelets.

## Discussion

With the application of confocal microscopy to the quantitative study of *in vitro* thrombus architecture[2], the development of high-speed confocal microscopy[3] and the use of laser-induced endothelial injury[1], we developed an intravital microscopy system to image thrombus formation in real time in the microcirculation of living mice. We used this instrumentation to explore the assembly of platelets, tissue factor and fibrin during thrombus formation in a living mouse.

Tissue factor is the initial activator of blood coagulation that culminates in the generation of a fibrin clot[4]. A membrane protein, it is expressed on most non-vascular cells[5,6]. The classical model has been that vascular injury leads to the exposure of flowing blood to tissue factor and rapid initiation of blood coagulation. Yet low levels of tissue factor circulate in normal plasma[7–9]. Nemerson used an *in vitro* thrombosis model, in which fresh human blood is perfused into a chamber to generate thrombi on collagen-coated slides or pig arterial medium, to show that tissue factor accumulates within the thrombus[10].

We observed platelet deposition, tissue factor localization and fibrin formation during thrombus formation in mice after defined vascular injury of the arterial vessel wall. We showed that tissue factor and fibrin were initially associated with the upstream aspect and vessel-wall interface of the thrombus, and propagated through the thrombus. Although observations of the confocal thrombus slices indicated that fibrin and tissue factor were distributed throughout much of the thrombus volume, tissue factor was concentrated at the thrombus–vessel wall interface. Indeed, some tissue factor was

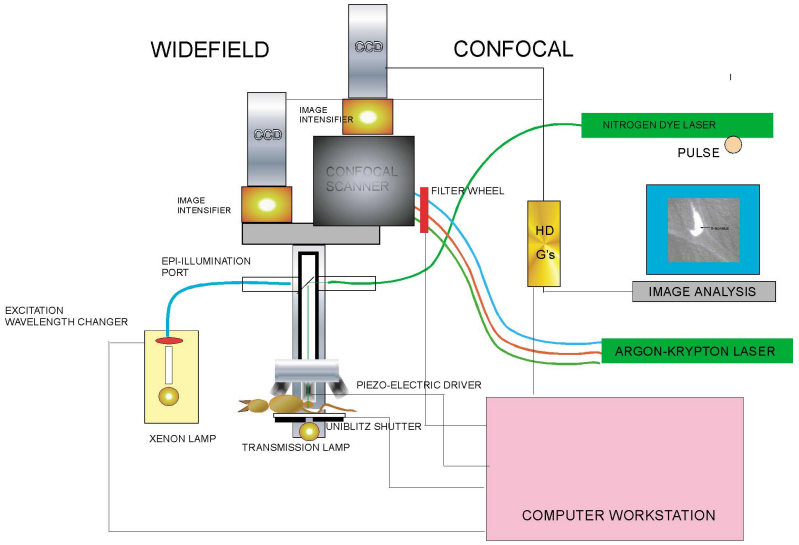


**Fig. 5** Schematic diagram of the confocal–widefield high-speed microscope used for real-time intravital microscopy of the microcirculation of a living mouse. For widefield applications, epi-illumination is delivered by repositioning the light path from a xenon lamp through one of 4 fixed excitation filters. Under computer control, excitation wavelengths can be changed as rapidly as every 1.2 ms. Images can also be collected in a brightfield channel controlled by the Uniblitz shutter. Light incident from the sample passes through an appropriate dichroic and emission filter, and the signal is enhanced by an image intensifier before being captured in the CCD camera. For confocal applications, a krypton–argon laser is filtered to deliver light of 488 nm, 568 nm or 647 nm. The plane of confocal illumination is changed by moving the objective lens by means of a piezo-electric motor under software control. The signal is also enhanced by an image intensifier before being captured in the CCD camera. Injury is initiated in the microvasculature by a nitrogen pulse dye laser. The light is coherent but not focused until it reaches the focal point of the objective; in this way light can be passed through intermediate tissue without damaging it. The confocal component is used to eliminate out-of-focus haze, to obtain 2-dimensional slices through the thrombus and to construct 3-dimensional optical images based upon stacking of image slices. The widefield microscope is used for the most rapid imaging, particularly when 4 channels are used. Exposure times are as short as 10–15 ms. Hard drive with ample gigabytes of storage.

## Methods

**Preparation of mice for intravital microscopy.** Mice were pre-anesthetized by intraperitoneal injection of ketamine, xylazine and atropine sulfate. Nembutal was administered through the jugular vein. The cremaster muscle was exteriorized in 4–7 min in preparation for intravital microscopy[11,12]. Antibodies in 200 µl of physiologic saline were infused through a jugular vein cannulus. All procedures were approved by the Animal Care and Use Committee of the Beth Israel Deaconess Medical Center.

**Laser-induced vessel-wall injury.** Between 5 and 60 min after antibody infusion, arterioles were identified and endothelial injury induced using a pulsed nitrogen dye laser at 440 nm applied through the microscope objective using the Micropoint laser system (Photonics Instruments, St. Charles, Illinois). Arterioles with a diameter of 30–60 µm were targets for injury. Multiple (6–10) independent experiments were done over the course of approximately 1 h.

**Antibodies and reagents.** To detect tissue factor, mice were infused with sheep antibody against rabbit tissue factor labeled with Alexa 488 (8 µg/g body weight; American Diagnostica, Greenwich, Connecticut), or with sheep IgG labeled with Alexa-488 (8 µg/g body weight) as a control. To detect fibrin, mouse antibody against the human fibrin IIβ chain (2 µg/g body weight; Accurate Chemical, Westbury, New York), or mouse $IgG_{1k}$ (2 µg/g body weight; BD Pharmingen, Palo Alto, California) as a control, were pre-incubated before infusion with goat antibody against mouse IgG conjugated to Alexa-488 (1 µg/g body weight). For some experiments, the fibrin antibody was directly labeled with Alexa-660 or Alexa-350. To detect platelets, rat antibody against mouse CD41 (0.1 µg/g body weight; BD Pharmingen), or rat $IgG_{1k}$ (0.1 µg/g body weight; BD Pharmingen) as a control, were pre-incubated before infusion with chicken antibody against rat IgG conjugated to Alexa-488 (1 µg/g body weight). As indicated, CD41 Fab fragments were labeled with Alexa-660. Alexa-350, Alexa-488 and Alexa-660 were conjugated to purified antibodies using the Alexa Fluor Protein Labeling Kit (Molecular Probes, Eugene, Oregon) according to the manufacturer's instructions. Fab fragments of antibodies were prepared using papain (Pierce, Rockford, Illinois) and were labeled with Alexa dyes.

**Intravital imaging.** We have designed a high-speed confocal and widefield microscope for intravital microscopy of the microcirculation of a living mouse (Fig. 5). This digital instrument allows near-simultaneous collection of images in up to 4 separate channels, each with a different fluorescence or brightfield image. We use an Olympus AX-70 fluorescence microscope with a long-distance condenser; a ×60 (NA 0.9) water-immersion objective is mounted on a piezoelectric driver and its controller to allow the focal plane to be rapidly changed.

For confocal fluorescence microscopy we used the Yokogawa CSU-10 confocal scanner (PerkinElmer, Gaithersburg, Maryland). This system is equipped with an argon–krypton 3-line laser for excitation at $\lambda_{ex}$ 488 nm, $\lambda e_x$ 568 nm, $\lambda_{ex}$ 647 nm and a Sutter Lambda L-10 filter wheel (Novato, California) on the excitation source. Widefield intravital microscopy was done using a Sutter Lambda DG-4 high-speed wavelength changer with a 175-watt xenon light source equipped with excitation filters (360 nm, 480 nm and 590 nm) matched to a triple-band filter for DAPI, FITC and Cy5 (Chroma, Brattleboro, Vermont) in the body of the microscope. To provide a brightfield channel while collecting image data in fluorescence channels, a Uniblitz (Vincent Associates, Rochester, New York) shutter supplied transmitted light. For both confocal and widefield imaging, light was amplified using a Videoscope (Sterling, Virginia) image intensifer. A Cooke SensiCam (Auburn Hills, Michigan) CCD camera (640 × 480 format) allowed the capture of up to 60 frames/s using 2 × 2 binning. A Dell workstation was used for synchronization of components, data acquisition and image analysis. SlideBook software (Intelligent Imaging Innovations, Denver, Colorado) was used for data capture, component control and image analysis. Statistical analyses were done using the Student *t*-test.

not co-localized with platelets but was adjacent to platelets along the vessel wall. These *in vivo* studies can be distinguished from the observations of Giesen *et al.*[10] who, on the basis of an *in vitro* model using human blood, posited that the propagation of blood coagulation might involve the accumulation of blood-borne tissue factor into the thrombus. Although blood-borne tissue factor may indeed be an important component of the developing thrombus, concentration of tissue factor along the thrombus–vessel wall interface and adjacent regions of the vessel wall points to the vessel wall itself as a source of, and required participant in, tissue-factor accumulation. Further studies using this new intravital technology and transgenic mice will address the origins of tissue factor. In addition, this instrumentation should be useful as a means to directly examine and quantify the anti-thrombotic activity of new pharmaceuticals and understand the pathogenesis of thrombi.

*Note: Supplementary information is available on the* Nature Medicine *website.*

*Acknowledgments*

*We thank S. Inoué for introducing us to the Yokogawa CSU-10 high-speed confocal microscope, Eric Furie for digital image capture advice, and F. Castellino and E. Rosen for demonstrating the laser injury model. This work was supported by grants from the US National Institutes of Health (HL51926 and HL69435). The confocal microscope was obtained with partial support from the National Institutes of Health (S10RR15680).*

*Competing interests statement*

*The authors declare that they have no competing financial interests.*

1. Rosen, E.D. *et al.* Laser-induced noninvasive vascular injury models in mice generate platelet- and coagulation-dependent thrombi. *Am. J. Pathol.* **158**, 1613–1622 (2001).
2. Savage, B., Almus-Jacobs, F. & Ruggeri, Z.M. Specific synergy of multiple substrate–receptor interactions in platelet thrombus formation under flow. *Cell* **94**, 657–666 (1998).
3. Inoue, S. & Inoue, T. (eds.). *Direct-view High Speed Confocal Scanner–the CSU-10* (Academic Press, New York, 2000).
4. Morrissey, J.H. Tissue factor: an enzyme cofactor and a true receptor. *Thromb. Haemost.* **86**, 66–74 (2001).
5. Morrissey, J.H., Fakhrai, H. & Edgington, T.S. Molecular cloning of the cDNA for tissue factor, the cellular receptor for the initiation of the coagulation protease cascade. *Cell* **50**, 129–135 (1987).
6. Spicer, E.K. *et al.* Isolation of cDNA clones coding for human tissue factor: primary structure of the protein and cDNA. *Proc. Natl. Acad. Sci. USA* **84**, 5148–5152 (1987).
7. Koyama, T. *et al.* Determination of plasma tissue factor antigen and its clinical significance. *Br. J. Haematol.* **87**, 343–347 (1994).
8. Fareed, J., Callas, D.D., Hoppensteads, D. & Bermes, E.W. Tissue factor antigen levels in various biological fluids. *Blood Coagul. Fibrinolysis* **6** (Suppl. 1), S32–S36 (1995).
9. Zumbach, M. *et al.* Tissue factor antigen is elevated in patients with microvascular complications of diabetes mellitus. *Exp. Clin. Endocrinol. Diabetes* **105**, 206–212 (1997).
10. Giesen, P.L. *et al.* Blood-borne tissue factor: another view of thrombosis. *Proc. Natl. Acad. Sci. USA* **96**, 2311–2315 (1999).
11. Ley, K. Gene-targeted mice in leukocyte adhesion research. *Microcirculation* **2**, 141–150 (1995).
12. Yang, J. *et al.* Targeted gene disruption demonstrates that P-selectin glycoprotein ligand 1 (PSGL-1) is required for P-selectin-mediated but not E- selectin-mediated neutrophil rolling and migration. *J. Exp. Med.* **190**, 1769–1782 (1999).